Effect of Exit Pressure of Steam Turbine Last Stage Cascade Blade on Two Phases of Saturated Vapor and Water Droplet

Dr. Assim H. Yousif
Machines & Equipments Engineering Department, University of Technology / Baghdad
Email: assim_yousif20000@yahoo.com
Dr. Amer M. Al-Dabbagh
Machines & Equipments Engineering Department, University of Technology / Baghdad
Reyadh Ch. Mahawi
Technical College, Foundation Technic/ Baghdad

ABSTRACT

Experimental investigation was carried out in low pressure steam turbine cascade to determine the effect of exit pressure on two phases of saturated vapor and fine water droplet. Numerical investigation was also presented by assuming the flow is two dimensional, compressible, turbulent, viscous, with the aid of the classical nucleation model applied for the mass transfer in the transonic conditions to predict the two phases behavior in the cascade. Comparison between experimental and theoretical results for the cascade flow was found to be fairly acceptable. Experimentally it was found that the most important influence of rapid condensation on the pressure distribution is on the suction surface. Also when the outlet is termed supersonic the heat release causes a pressure rise in the zone of rapid condensation, therefore the term "condensation shock" for this feature is misleading. In the numerical approach when the flow is regard subsonic the rapid condensation zone occurs downstream the throat and not accompanied by a pressure rise, while in the experimental test for the same case there is no sign of this condensation.

Keywords: cascade, condensation, two phases, saturated, vapor, droplet, exit pressure.

تأثير ضغط الخروج لصف من رش المراحل الاخيرة لتوربين بخاري على طورين من البخار المشبع وقطرات ماء

الخلاصة

اجري اختبار تجريبي في صف من ريش توربين بخاري ذي ضغط واطيء لتحديد تاثير ضغط الخروج على طوري البخار المشبع وقطرات الماء الصغيرة. بفرض ان الجريان ذو بعدين انضغاطي اضطرابي لزج وبمساعدة نموذج التكاثف التلقائي المتجانس الكلاسيكي المطبق على

235

حالة انتقال الكتلة في ظروف حول الصوتي فان الحل العددي تم تقديمه أيضا للتنبؤ عن سلوك الطورين في صف ريش.

بينت المقارنة بين النتائج التجريبية والعددية لجريان صف الريش بوجود توافق مقبول, تجريبيا وجد ان التأثير المهم للتكثيف السريع على توزيع الضغط يكون عند سطح المص. كذالك عندما تكون الظروف عند الخروج فوق الصوتي فان طرح الحرارة يؤدي الى زيادة الضغط في مكان التكثيف السريع لذلك فان الحد المتعارف عليه والذي يعرف بحد الصدمة لا ينطبق على هذه الحالة. أما في الجانب العددي وعندما يعد الجريان دون الصوتي فان مكان حدوث التكثيف يحدث اسفل العنق ولايواكبه زيادة في الضغط في حين ولنفس الحالة في جانب الاختبارات العملية لاوجود لأي اشارة لهذا التكثيف في منطقة اسفل العنق.

INTRODUCTION

The great majority of power stations the steam supplied to the turbines are superheated, but in the course of expansion through the machine its state path crosses the saturation line and some of the stages have to operate on wet steam and an appreciable fraction of the power is generated in the wet stages. This stages have comparatively lower efficiencies and the phenomena contributing to the increased losses are insufficiently understood, So that the modeling of wet steam is very important in the analysis and design of steam turbines, because the low-pressure turbine stages are of especial importance because of their relatively large generation of power, they are prone of the influence of additional losses induced by condensation [1].

Many experimental investigations for the performance of the last stages of turbines do not offer a satisfactory means. This is related to investigate the influence of the individual factors that contribute to wetness losses. Also because of most of the pervious testing has been performed in air due to extra difficulties associated with contamination of instrumentation and flow visualization by condensation and long thermal settling time between condition changes.

EXPERIMENTAL INVESTIGATION

The experimental work was conducted to provide means for validating the theoretical prediction of wet steam nucleation and to understanding the mechanism that cause the extra losses due to nucleation. To reproduce turbine nucleating and wet flow conditions, requires a supply of supercooled steam; this can be achieved under blow-down facility by the equipment employed (steam turbine) according to [2], in which the results confirm that nucleating flows exhibit features that are absent from superheated flows. A general description and discussion of the results of the experiments of the last stage stator blade are given by [3].

The quality of the measurements, particularly, the Schlieren photographs of the trailing edge Shock-wave system were extremely high. This provided an extensive set of data, both for validation of the computer codes and for studying the operation of a full-sized cascade under genuine wet-steam conditions.

Therefore at the present work experimental study was accomplished for non equilibrium condensing transonic steam flow in a stationary cascade of last stage stator turbine blade. The conditions at inlet to the test section could be varied from a wet equilibrium to a superheated state by adjusting the cascade exit pressure.

Eng. & Tech. Journal, Vol.31, No.2, 2013   Effect of Exit Pressure of Steam Turbine Last
Stage Cascade Blade on Two Phases of
Saturated Vapor and Water Droplet

Shadow graph technique is introduced to photographs the trailing edge Shock-wave system and the condensation zone. The real conditions of the last stages of steam turbine are ranging between 0.5 and 0.35 bars absolute and 75-82 ℃. This condition is produced by using expansion drum technique. The drum is designed and constructed to obtain inlet vacuum pressure to supply supercooled steam to the cascade test rig. Static pressure measurements on both cascade blade surfaces and at the mid distance of the cascade passages were also done.

EXPERIMENTAL FACILITIES

The general arrangement and main components of the expansion drum facility are shown diagrammatically in figure (1). Steam was supplied to the test section from boiler via throttling valve, flow regulation valve and expansions drum. The steam conditions at inlet to the test section can be varying from a wet equilibrium to a superheated state by adjusting the water pass through the boiler and amount of steam entering and leaving the expansion drum. The flow leaving the test section is passing to a condenser, by varying the cooling water flow rate in the condenser and vacuum pump, therefore the test section pressure ratio and hence the exit Mach number can be controlled.

One of the problem rises in this research is how to obtain steam of properties for last stage of steam turbine which is of vacuum pressure down to 0.5 bars or may be less and temperature range of 75 to 82 ℃. The present laboratory facility contained of steam boiler of 10 bars combined with steam turbine of single stage impulse turbine where the steam expanded from 10 bars to 0.5 bars absolute. The preliminary results showed that a great amount of steam energy spend by driving the turbine with process of high expansion and condensation rate. For the previous reason an expansion drum has been used instead of the turbine to overcome the high expansion rate of the steam, and to obtain the required amount, pressure, temperature and condition of the steam (i.e. steam at zone close to saturation vacuum pressure).The drum also has many functions such that it work as settling chamber that absorb steam flow disturbance and pressure fluctuating that exit from the orifices tube of the expansion drum. This process leads to obtain uniform flow in test section. The drum size was selected suitable large enough to satisfy the above requirements. The drum has a cylindrical shape with two ended cups. The drum diameter is 0.9 m and the drum height is 2 m with addition of the two ended cups gave 1.271 m^3 total sizes. For more details see [4].

CASCADE TEST SECTION

To obtain uniform flow the inlet of the test section is constructed from two longitudinal parts. The first part is of convergent cross section, the second part of parallel side with exit dimensions identical to the test section cross sectional area. The depth of the test section was 26 mm, giving a blade aspect ratio of 1.1 and to ensure a reasonable two dimensional flow field at the mid-plane of the passage [5]. The test section was staggered by an angle of (45.32°) to simulate the real steam turbine blade staggered angles. This may help to avoided contamination of the shadowgraph window with coarse water, enabling clear visualization of the trailing edge shock waves. The mass flow rate available from the boiler limited the number and size of blades to four, thus providing only three passages. This is the minimum

number that could be used for an acceptable validation of computer code incorporating periodic boundary condition modeling a finite cascade [3]. The blade profile selected for the experiments is a geometrical copy of a fifth stage stator blade from the six-stage low pressure steam turbine. This profile is chosen because experiments previously conducted in the actual turbine had indicated high losses in the fifth stage which corresponded to the location of the primary nucleation. Also a comparison between the identical present and existing results of [2] and [3] can be done easily. The exit design Mach number was 1.2 and the outlet flow angle about 71°. All the characteristic values of cascade can be evaluated as listed in Table (1).

Table (1) characteristic values of cascade.

Blade axial chord	23.07 mm
Blade pitch	21.8 mm
Blade chord	32.8 mm
Stagger angle	45.32º
Inlet flow angle	0.0º
Outlet flow angle	71.0º
Solidity	1.5
Span or blade height	26 mm
Aspect ratio	1.1
Throat	7.1 mm

The three blade passages were formed from two blades and two half profile blades. The two half profile blades were machined from aluminum blocks. The upper and lower halves represent the pressure and suction surfaces of the blade respectively. The two sides of the test section was constructed from 10 mm thickness pure glass to permit a clear vision of the physical changed in the fluid properties especially at the trailing edge region. Figure (2) shows the cascade test section arrangement.

To carry out the surface pressure measurements, tapping were drilled into the blade surfaces (pressure and suction) as shown in figure (3); also the wall tapping were drilled along the middle passage line starting from upstream to downstream of the cascade. The measuring points of the static pressure at the middle of the cascade passage gave pressure distribution along the mid span of the passage. This pressure distribution gave a clear picture of the Mach number distribution along the middle passage. Pressure lines were lead out from the test section via steel tubing contained within cascade frame and measurements were made using a multi tube manometer connected to the tapings by a scans valve arrangement. For more details see [4].

THE SHADOWGRAPH TECHNIQUES

This technique was used for observing flow field; it is particularly useful where there are large density gradients, such as in flow across a shock wave. The schematic diagram of equipment used in this technique is shown in figure (4).Source of light is fixed on one side of working section in the direction normal to glass window, the concave lens is located in front of the laser source to enlarge the laser beam, and then the laser beam passes through convex lens located in front

Eng. & Tech. Journal, Vol.31, No.2, 2013   Effect of Exit Pressure of Steam Turbine Last
Stage Cascade Blade on Two Phases of
Saturated Vapor and Water Droplet

of concave lens, so that the light parallel beam will cover the area of the test section. The light beam penetrating the test section falls on the mirror inclined to reflect on the white photograph plate. A digital camera is used to capturing the image.

NUMERICAL INVESTIGATION

A number of numerical studies were directed toward modeling two phase flow behavior of nucleating steam. Much of this modeling work was initially conducted on two dimensional flows in turbine cascade; in this regard the numerical approaches most often used have been the single phase, inviscid, and time-marching scheme of Denton for turbo machinery flows as done by **[6]** and **[7]**. Using these approaches gives limitations on extending these methods to more complex flow conditions involving nucleation steam. With more sophisticated numerical models used contains the viscous and turbulence effects as made by **[8]** and [9]. Therefore additional information about two phase flow behavior of nucleating steam can be achieved.

At the present work attention is restricted to the behavior of homogeneous nucleation. The equations governing droplet nucleation and growth can be combined with the field conservation equations and the behavior of nucleating and two-phase flows analyzed. The Eulerian–Eulerian approach was adopted for modeling the condensing steam flow. And the two-phase flow is modeled using the conservation-type two-dimensional compressible Navier-Stokes equations, with the transport equations for the liquid-phase mass fraction and the number of liquid droplets per unit volume. Under the foregoing assumptions, the mixture flow is governed by the compressible Navier-Stokes equations. The mixture pressure, temperature and velocity components are obtained by solving Navier-Stokes equations using a second-order spatially accurate density–based flow algorithm. This algorithm employs a coupled algebraic multigrid to accelerate a two-sweep point implicit Gauss-Seidel relaxation scheme.

To model wet steam, two additional transport equations are needed. The first transport equation governs the mass fraction of the condensed liquid phase (β) and the other transport equation (η) determines the number of droplets per unit volume. The two equations are combined to the model in the following expression:

$$\frac{\partial \rho}{\partial t}\beta + \nabla.(\rho\vec{v}\beta) = \Gamma \qquad \qquad \dots (6)$$

$$\frac{\partial \rho}{\partial t}\eta + \nabla.(\rho\vec{v}\eta) = \rho I \qquad \qquad \dots (7)$$

Where Γ is the mass generation rate due to condensation and evaporation (kg per unit volume per second).and I is the nucleation rate (number of new droplets per unit volume per second).

The number of droplets per unit volume given by the following expression:

$$\eta = \frac{\beta}{(1-\beta)V_d(\rho_l/\rho_g)} \qquad \qquad \dots (8)$$

Average droplet volume (V_d) is defined as

Eng. & Tech. Journal, Vol.31, No.2, 2013   **Effect of Exit Pressure of Steam Turbine Last**
Stage Cascade Blade on Two Phases of
Saturated Vapor and Water Droplet

$$V_d = \frac{4}{3}\pi\bar{r}^3 \qquad\qquad \dots(9)$$

$\bar{r}$ is the average droplet radius

The mass generation rate Γ in the classical nucleation theory during the nonequilibrium condensation process is given by the sum of mass increase due to nucleation (the formation of critically sized droplets) and also due to growth/demise of these droplets.

Therefore, Γ is written as:

$$\Gamma = \frac{4}{3}\pi\rho_l I r_*^3 + 4\pi\rho_l\eta\bar{r}^2\frac{\partial\bar{r}}{\partial t} \qquad\qquad \dots(10)$$

r_* is the Kelvin-Helmholtz critical droplet radius, above which the droplet will grow and below which the droplet will evaporate. Expressions for $r_*, I\ and\ \frac{\partial\bar{r}}{\partial t}$ is given by:

$$r_* = \frac{2\sigma}{\rho_l RT_g \ln S} \qquad\qquad \dots(11)$$

and

$$I = \frac{q_c}{1+\nu}\frac{\rho_g^2}{\rho_l}\left(\frac{2\sigma}{\pi m^3}\right)^{\frac{1}{2}}\exp\left(-\frac{4\pi\sigma r_*^2}{3kT_g}\right) \qquad\qquad \dots(12)$$

and

$$\nu = q_c\frac{2(\gamma-1)}{(\gamma+1)}\frac{h_{lg}}{RT_g}\left(\frac{h_{lg}}{RT_g} - 0.5\right) \qquad\qquad \dots(13)$$

and

$$\frac{d\bar{r}}{dt} = \frac{PC_p}{\rho_l h_{lg}\sqrt{2\pi RT_g}}\frac{(\gamma+1)}{2\gamma}(T_l - T_g) \qquad\qquad \dots(14)$$

NUMERICAL MODEL

At the present numerical investigation the calculations were performed for various flow conditions similar to the experiments covering subsonic, sonic and supersonic dry and nucleating flows.

The numerical model presented here will be used to investigate the nucleation of steam with the effects of viscous and turbulence using a CFD code Fluent 12.1. This model as described in section (6) is implemented within a full Navier–Stokes viscous flow solution procedure, employs a density based finite volume discretization of the governing equations of fluid motion.

The RNG-based $(k - \varepsilon)$ turbulence model derived from the instantaneous Navier-Stokes equations was used in the CFD code as recommended by **[10]**. The analytical derivation results in a RNG-based $(k - \varepsilon)$ model with constants different from those in the standard $(k - \varepsilon)$ model, and additional terms and functions in the

transport equations for (k) and (ε). A more comprehensive description of RNG theory and its application to turbulence can be found in [11]. Two dimensional structured meshes quadrilateral were selected to define the grid generation and the grid close to the leading and trailing edges were refined. The pressure and suction sides of the blade should also be adequately clustered. The grid generation for cascade passage is shown in figure (5).

In the two dimensional case a correct definition of boundary conditions are needed. In addition to inlet and outlet boundary conditions, the solid wall and periodic boundary which are necessary for calculation of flow through a turbine blade cascade as shown in figure (6).

RESULTS AND DISCUSSIONS

Comparisons between calculated and measured results are presented in Figures (7) to (9). The speed of sound in a two phase mixture is not explicit, and it values depends on the local conditions, while the pressure can be directly measured. For this reason in two phase flows it is preferable to work in terms of static pressure ratio (P_s/P_o), therefore the isentropic Mach number can be based on this ratio. Static pressure ratio and isentropic Mach number distributions for blade pressure and suction sides and mid passage distance are shown in these Figures. It can be seen that these Figures show well agreement between calculated and measured results

Typical shadowgraph photos of the cases, that the conditions at inlet to the test section could be varied from a wet equilibrium to a superheated by changing the back pressure, are used to compare the flow structure and trailing edge shock wave system with the theoretical isentropic Mach number and droplets growth rate contours as shown in figures (10) to (12). The condensation zone, the area of the propagation of dark region inside the dotted line envelope occurred downstream the throat area due to the reduction of the back pressure. This condensation process is increasing the rate of expansion, the departures from thermodynamic equilibrium, that lead to release latent heat from the droplets. When the outlet flow is supersonic the heat release from the droplets causes a pressure rise in the zone of rapid condensation in the blade suction side, the dark zone in the shadowgraph photos as shown in Figures (11-c) and (12- c). The same analysis is also mentioned by [12].

Figure (13) shows the variation in liquid mass fraction in the computational domain. Low back pressure causes high liquid mass fractions. As the rate of expansion increased a results of more departures from thermodynamic equilibrium and the superheated steam crosses the saturation line and becomes saturated. It can be seen from these figures that the liquid mass fraction have a low values of order of 10^{-8}, since the outlet flow either to be subsonic or sonic as shown in Figure (13-a), this due to the steam is remains in superheated zone; therefore there is no departure from thermodynamic equilibrium or nearly so.

Figure (14) shows that the computed droplets nucleation rate is increased as the back pressure decreased. The droplets nucleation rate occurred downstream away of the throat and move toward the throat as the back pressure is decreased. The position of the maximum values of the droplets nucleation rate is mostly occurred downstream the throat in the rapid condensation zone and continuing increasing in high rate with continuing decreasing the back pressure.

Figure (15) shows the variation in subcooled vapor temperature in the computational domain at different values of back pressure. This figure show that the reduction in back pressure for different range of inlet superheat resulting in increasing the subcooled vapor temperature. This increment is attributed to condensing flow of steam. The steam can be regarded as a special case of compressible fluid flow with heat addition in which the source is the latent energy released by phase change from steam to droplet water that releases latent heat, in the same time the water droplet growth continue growing, as a result of this growth both the subcooling and nucleation is decreased. This can be explained by criteria that this reduction may be occurred due to the latent heat created by the nucleation process is equal to the accelerating effect of flow caused by the divergent shape of the cascade passage. The maximum value of droplets subcooled vapor temperature takes place downstream the throat at the position of rapid condensation and is called "Wilson point" (x= 0.94-0.96) according to [3]. The subcooled vapor temperature (i.e. $\Delta T_{subcooled}$) has values less than 30 °K when the flow termed sonic and subsonic and greater than 30 °K in supersonic flow.

Figure (16) shows the variation in total temperature in the computational domain at different values of back pressure. This figure shows that in the subsonic cases, there are very small increments in total temperature order of (1-3 °K). This can be easily attributed to very small heat release from the droplets in subsonic flow, so that the droplets nucleation rate and droplet growth rate are also very small.

On other hand, at supersonic cases it was found that the increasing in total temperature is high, order of (30 to 40 °K). This may be attributed to high rate of expansion occurred with reduction of back pressure that leads to increases the heat release from the droplets. As a matter of fact the droplet nucleation rate and droplet growth rate are also increased to higher values. The total temperature values at the trailing edge shock region on suction side also increased and then start to decrease downstream the shock location. Also it was found that there is no effect on the total temperature behavior, when the inlet superheated conditions variation is taken into account at the shock region, while the total temperature is decreased just after the shock.

CONCLUSIONS

The present experimental results have given available data that validate the theoretical procedure employed. In general the comparison between experimental and theoretical results for the cascade flow was found to be fairly acceptable. The most important influence of rapid condensation on the pressure distribution is experienced on the suction surface. But in the numerical results when the flow is regard subsonic flow the rapid condensation zone still occurs downstream the throat and not accompanied by a pressure rise, while in the experimental shadowgraphs photos for same case there is no indication of this condensation. When the outlet is termed supersonic, the heat release causes a pressure rise in the zone of rapid condensation, which shows up in shadowgraph photos as a dark zone. However, the use of the term condensation shock for this feature is misleading.

The dominant effect of phase change in high speed condensing flows is the local departures from thermodynamic equilibrium associate with the sudden release

of heat, in which the system subsequently recovered. The internal heat transfer associated with phase change is thermodynamically an irreversible process. It is particularly dramatic during the nucleation process that incurs an entropy increase associated with increase in stagnation temperature and hence a loss in work potential.

REFERENCES
[1]. Dobes, J. J. Fort and J. Halama: (Numerical solution of single and multi-phase internal transonic flow problems). International Journal for Numerical Methods in Fluids, Vol.48, pp.91-97.(2005).

[2]. Bakhtar, F. M. Ebrahimi and R.A. Webb: (on the performance of a cascade of turbine rotor tip section blading in nucleating steam, part 1: surface pressure distributions), Proc. Instn. Mech. Engrs., Vol. 209, pp. 115-124. (1995).

[3].White, A.J. J.B. Young and P.T. Walters:(Experimental validation of condensing flow theory for a stationary cascade of steam turbine blades), Phil. Trans. Roy. Soc. Series A, 354, pp.59-88, (1996).

[4].Mahawi R. C.: (Experimental and numerical simulation of spontaneously condensing flow in turbine cascade). Ph. D. Thesis, University of Technology, Iraq (2012).

[5]. Cohen, H. G.F.C. Rogers and H.I.H. Saravanamutto: (Gas turbine theory) 4th edition, Book by Longman Group Limited, England, (1996).

[6]. Zamri; M.Y. H. Ibrahim and M.I. Azree: (Prediction and Improvement of Steam Turbine Performance Using Computational Fluid Dynamics), Department of Mechanical Engineering College of Engineering University Tenaga Nasional (UNITEN), (2000).

[7]. Zori and F. Kelecy L.:(Wet Steam Flow Modeling in a General CFD Flow Solver), 35th AIAA (American Institute of Aeronautics and Astronautics) Fluid Dynamics Conference pp.1-15, (2005).

[8]. Yusoff and T.F. Yusaf K.C. Ng, M.Z.: (Simulation of Two-dimensional High Speed Turbulent Compressible Flow in a Diffuser and a Nozzle Blade Cascade), American Journal of Applied Science 2, Vol. 9, pp. 1325-1330, (2005).

[9]. Ebrahimi and M. H. Roozbahani M.: (Numerical Investigation of Nucleating Flows of Steam in a Cascade of Turbine (Effect of Overall Pressure Ratios)), Majlesi Journal of Mechanical Engineering, Vol. 3, No. 4, (Summer 2010)

[10]. Yousif and H. Tarteb A.H.: (Validation of numerical computations and turbulence models combinations for gas turbine cascade blade flow), Engineering and Technology Journal, Vol.29, No.14 (2011).

[11]. Choudhury D.: (Introduction to the Renormalization Group Method and Turbulence Modeling), Fluent Inc. Technical Memorandum TM-107, (1993).

[12]. Mashmoushy, H. M.R. Mahpeykar and F. Bakhtar: (Studies of nucleating and wet steam flows in two-dimensional cascades), Proceedings of the Institution of Mechanical Engineers, Part C, Journal of Mechanical Engineering Science, Vol.218,(2004).

NOMENCLATURE
Roman symbols

C_P	Specific heat capacity, kJ/kg.K.
$\dfrac{d\bar{r}}{dt}$	Droplet growth rate.
h_{lg}	Specific enthalpy of evaporation (Latent heat), kJ/kg.
I	Nucleation rate, No. nuclei/m^3.s.
k	Turbulent kinetic energy, m^2/s^2.
m	Mass of a condensable vapor molecule, kg.
P	Pressure, bar.
q_c	Condensation coefficient.
r	Droplet radius, m.
R	The gas constant per unit mass, kJ/kg.K.
S	Saturation ratio.
T	Temperature, K.
V	Velocity, m/s.
V_d	Average droplet volume, m^3.
x/c_x	Fraction of surface distance.

Greek symbols

β	The wetness mass fraction.
Γ	Mass generation rate due to condensation and evaporation, Kg/m^3.s.
γ	Ratio of specific heat capacities.
η	Number of liquid droplets per unit volume.
ε	Dissipation of Turbulent Kinetic Energy, m^2/s^2.
ρ	Density, kg/ m^3.
σ	Surface tension, N/m.

Subscript and Superscript

g	Gas.
in	Inlet boundary conditions.
l	Liquid.
o	Stagnation or Total conditions.
*	Critical.
-	Average.

Eng. & Tech. Journal, Vol.31, No.2, 2013

**Effect of Exit Pressure of Steam Turbine Last
Stage Cascade Blade on Two Phases of
Saturated Vapor and Water Droplet**

Part No.	Description
1	Water softener
2	Cold water tank
3	Steam generator
4	Throttling valve
5	Steam flow regulation valve
6	Expansion drum
7	Orifices tube
8	Test section
9	Vacuum pump
10	The condenser
11	Water pump
12	Cooling tower

Figure (1) A schematic diagram of the system.

Figure (2) test section dimensions.

Eng. & Tech. Journal, Vol.31, No.2, 2013   Effect of Exit Pressure of Steam Turbine Last
                                                              Stage Cascade Blade on Two Phases of
                                                              Saturated Vapor and Water Droplet

Figure (3) the wall tapping points in the blade surfaces.
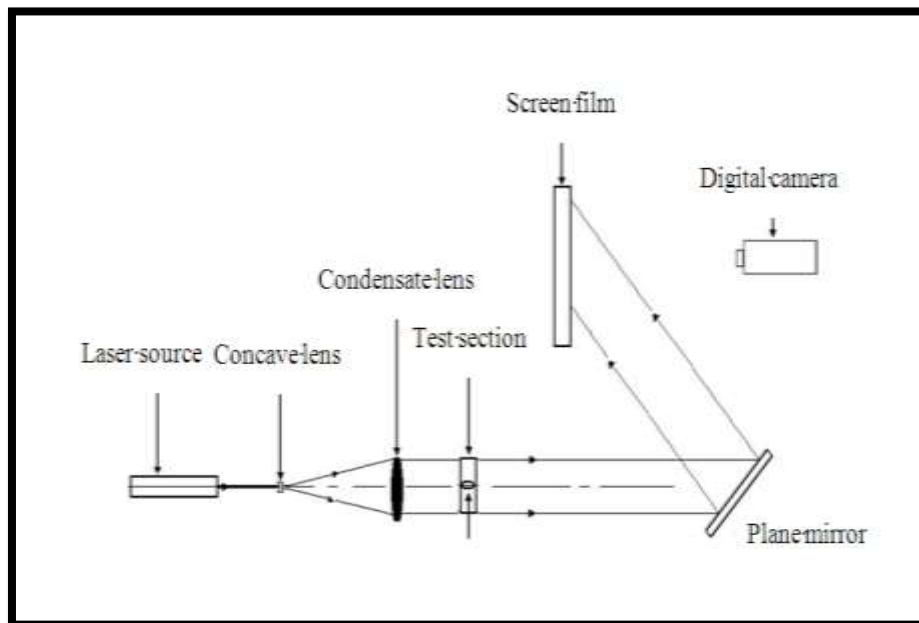
Figure (4) a schematic diagram of shadowgraph technique
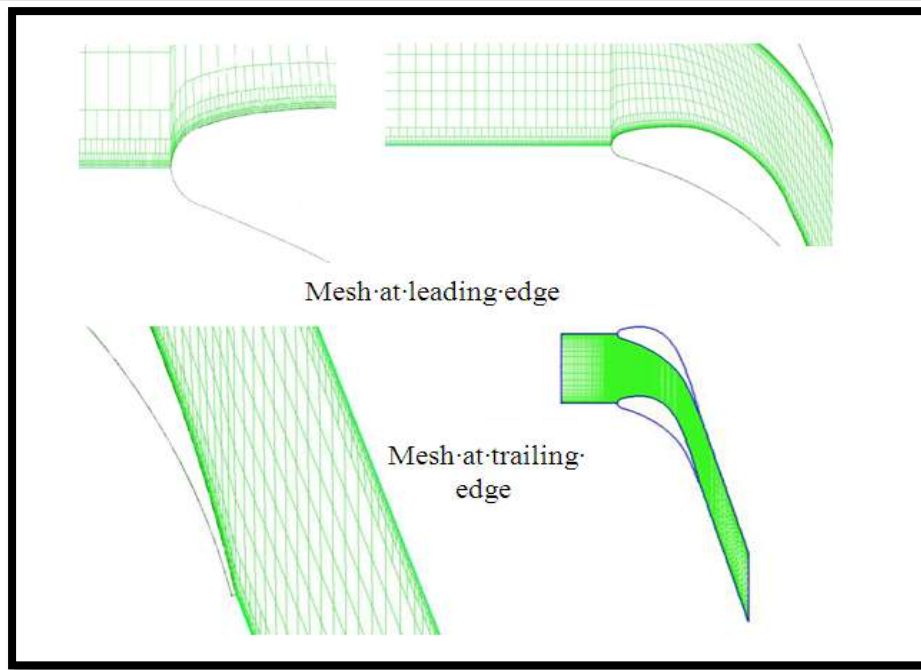
Figure (5) the computational domain
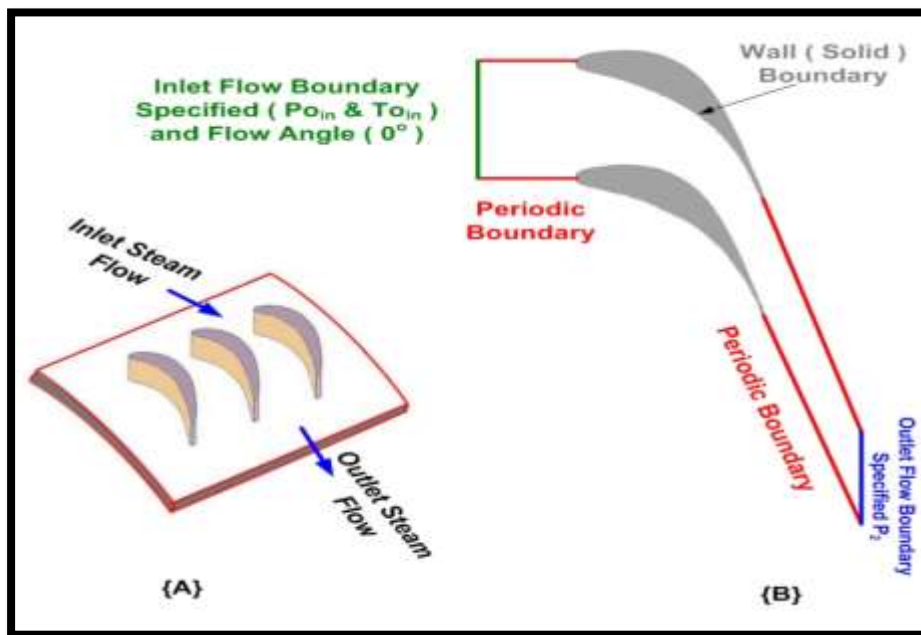
Figure (6) {A} Schematic draw of a row of stator set of turbine blades {B} Blade geometry and computational domain and boundary conditions for the stator blade cascade of an axial turbine.
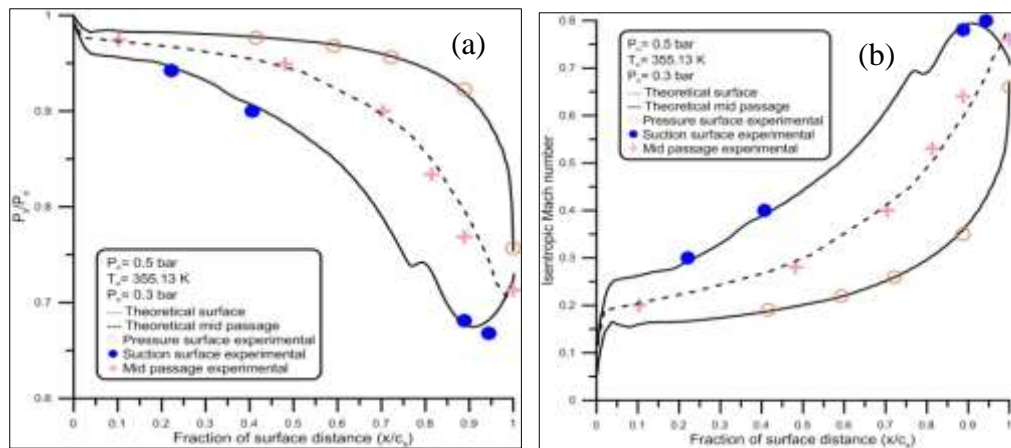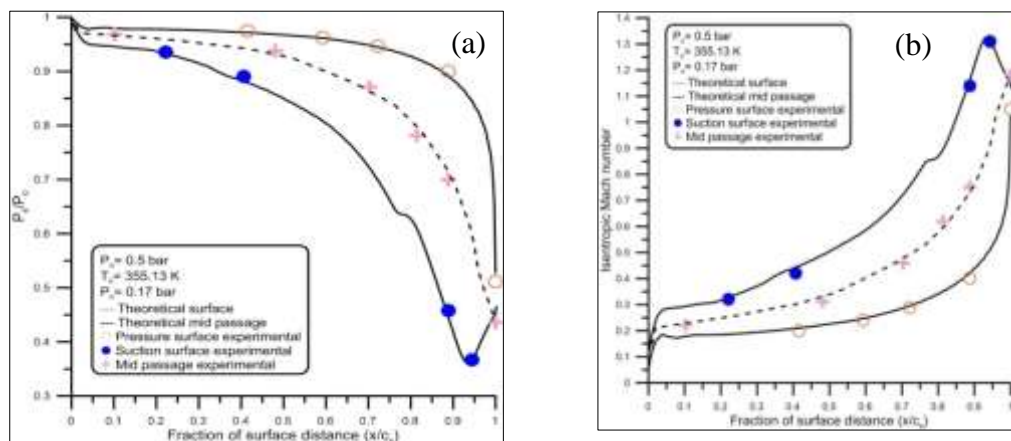
Figure (7) variation of (a) blade surface static pressure ratio, (b) Blade surface isentropic Mach number with fraction of surface distance.
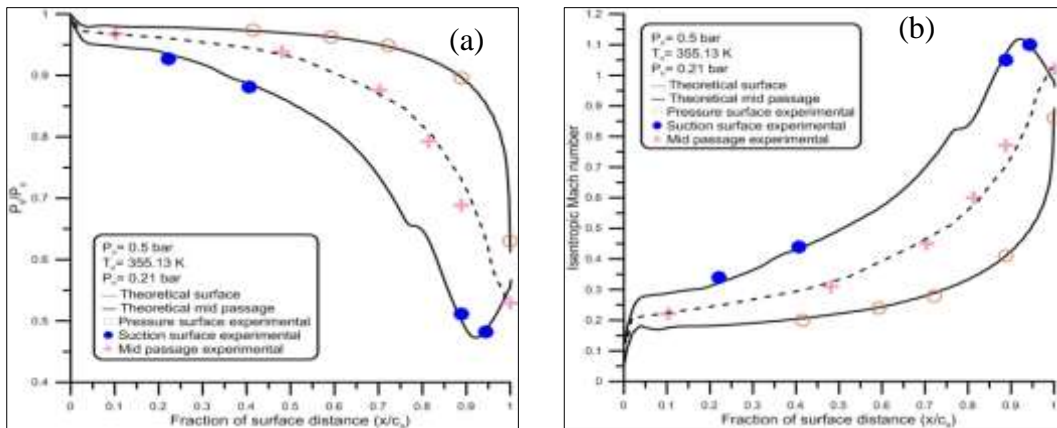
Figure (8) variation of (a) blade surface static pressure ratio, (b) Blade surface isentropic Mach number with fraction of surface distance.

Figure (9) variation of (a) blade surface static pressure ratio, (b) Blade surface isentropic Mach number with fraction of surface distance.
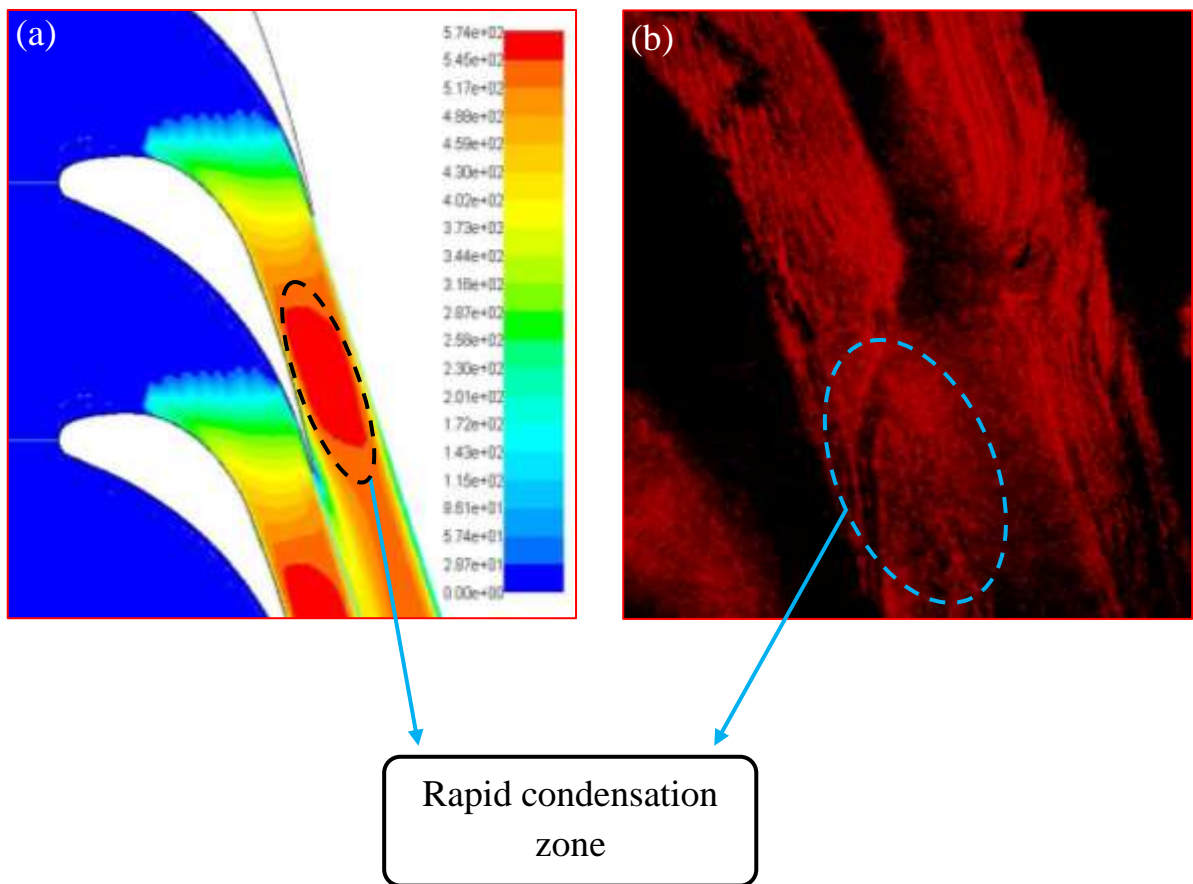
Figure (10) test No. 1. (P_o= 0.5 bar, T_o= 355.13 K, P_b= 0.3 bar), (a) predicted droplet growth rate contour (micron/s) and (b) shadowgraph photo.

Eng. & Tech. Journal, Vol.31, No.2, 2013

Effect of Exit Pressure of Steam Turbine Last Stage Cascade Blade on Two Phases of Saturated Vapor and Water Droplet
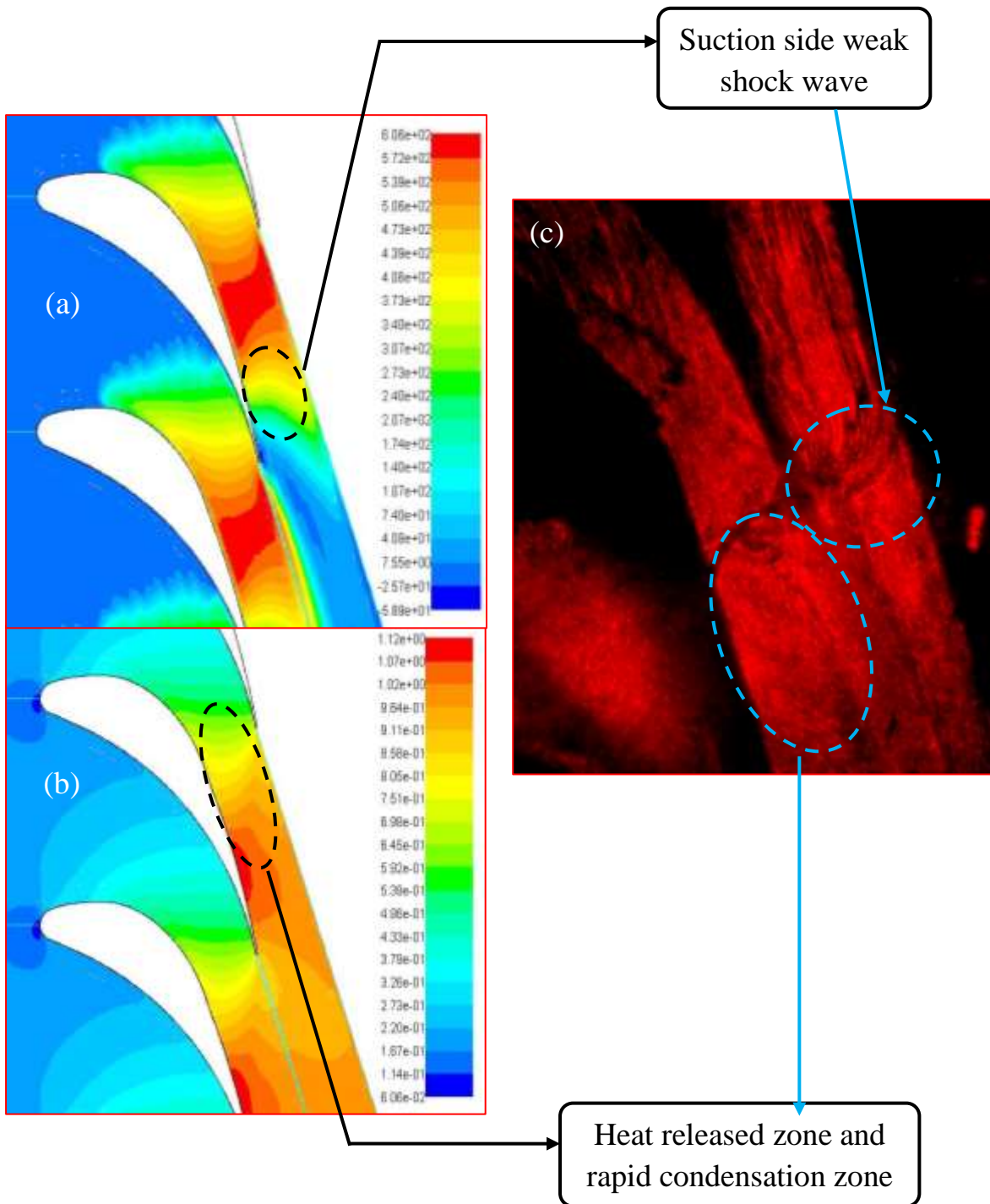
Figure (11) test No.2 (P_o= 0.5 bar, T_o= 355.13 K, P_b= 0.21 bar) (a) Predicted isentropic Mach number contour, (b) predicted droplet growth rate contour (micron/s) and (c) shadowgraph photo.
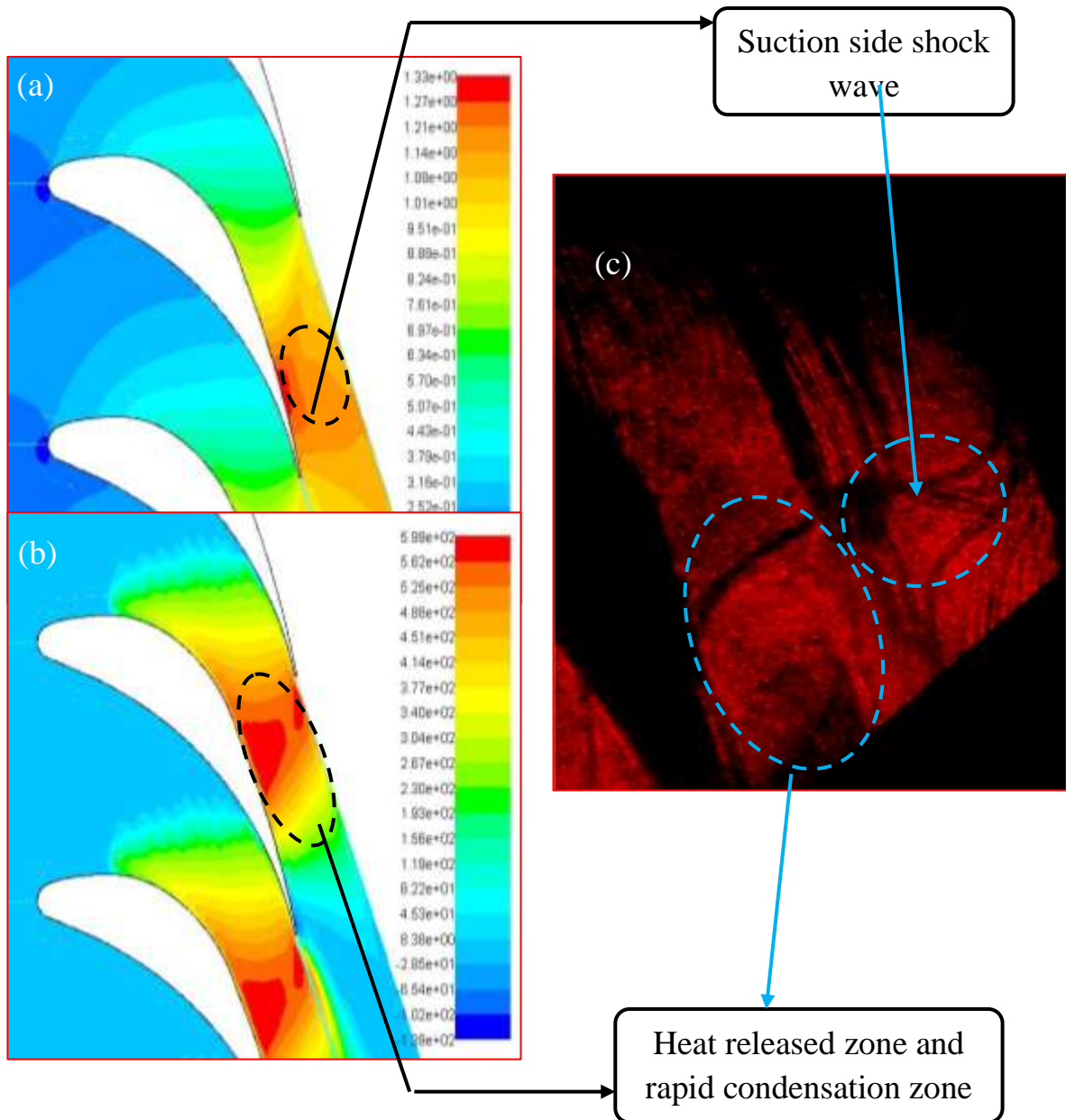
Eng. & Tech. Journal, Vol.31, No.2, 2013

Effect of Exit Pressure of Steam Turbine Last
Stage Cascade Blade on Two Phases of
Saturated Vapor and Water Droplet

Figure (12) test No. 3 (P$_o$= 0.5 bar, T$_o$= 355.13 K, P$_b$= 0.17 bar),
(a) Predicted isentropic Mach number contour, (b) predicted droplet
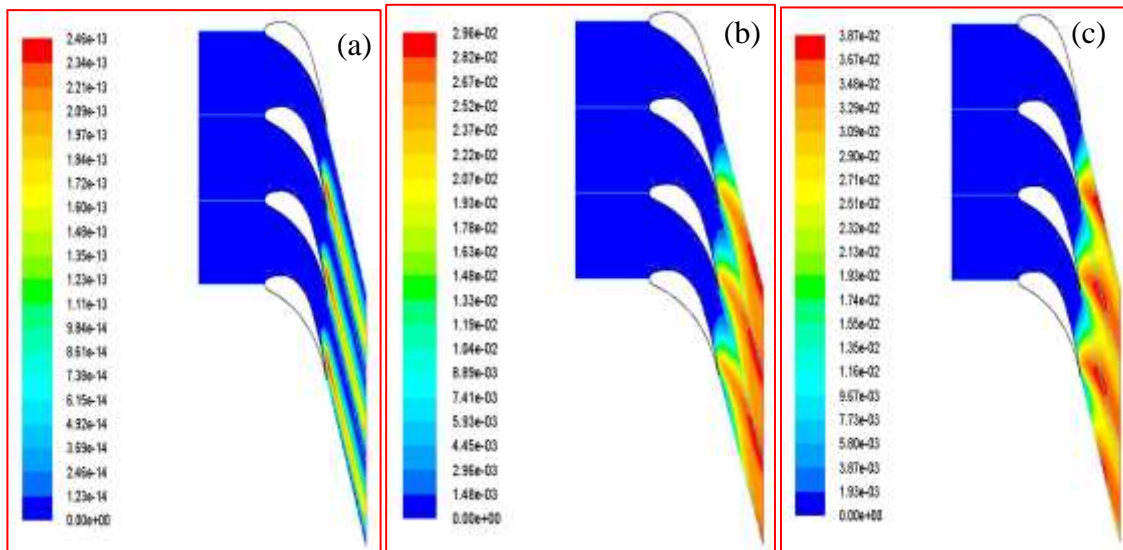growth rate contour (micron/s), and (c) shadowgraph photo.

Eng. & Tech. Journal, Vol.31, No.2, 2013

Effect of Exit Pressure of Steam Turbine Last Stage Cascade Blade on Two Phases of Saturated Vapor and Water Droplet

Figure (13) liquid mass fraction contours at (P_o= 0.5 bar, T_o= 355.13 K) and different back pressure ((a) P_b= 0.3 bar, (b) P_b= 0.21 bar, (c) P_b= 0.17 bar).

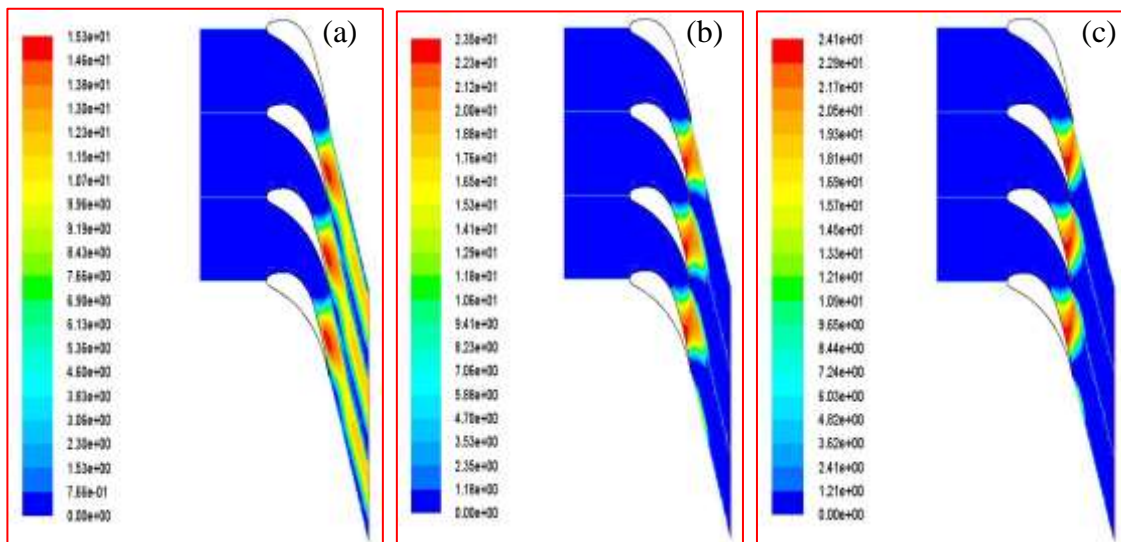**Figure (14) $\log_{10}$ droplets nucleation rate contours at (P_o= 0.5 bar, T_o= 355.13 K) and different back pressure ((a) P_b= 0.3 bar, (b) P_b= 0.21 bar, (c) P_b= 0.17 bar).**

Eng. & Tech. Journal, Vol.31, No.2, 2013 Effect of Exit Pressure of Steam Turbine Last
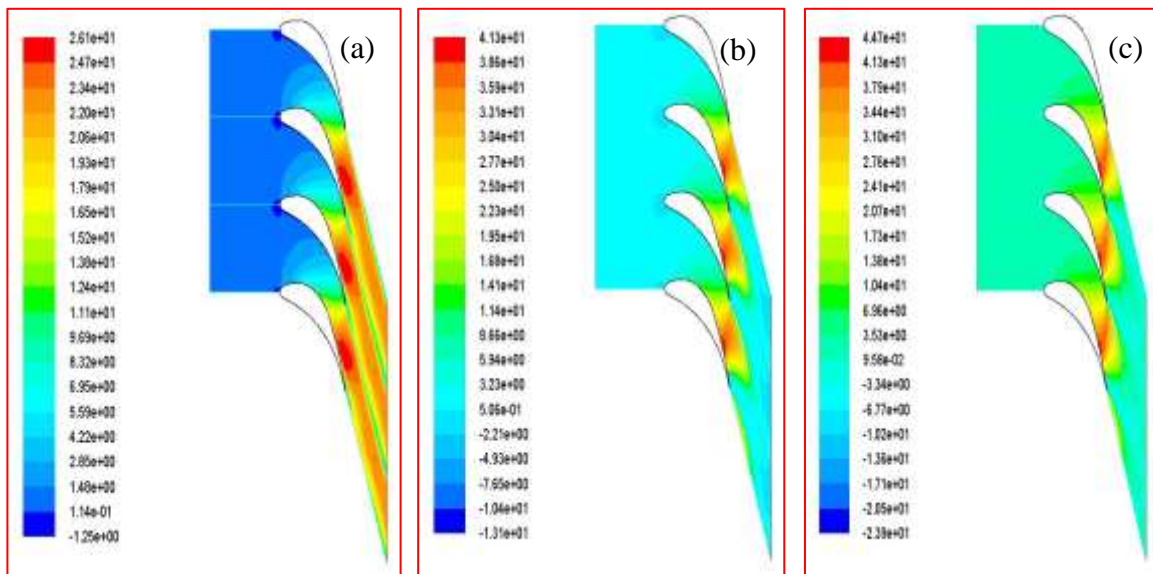Stage Cascade Blade on Two Phases of
Saturated Vapor and Water Droplet

**Figure (15) subcooled vapor temperature contours (K) at (P_o= 0.5 bar, T_o=
355.13 K) and different back pressure ((a) P_b= 0.3 bar, (b) P_b= 0.21 bar, (c)
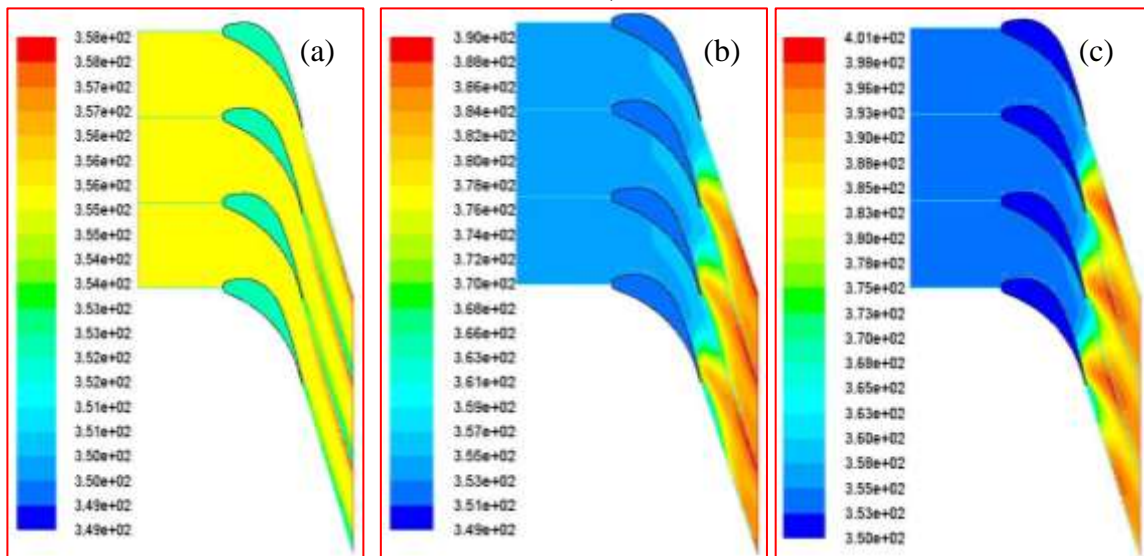P_b= 0.17 bar).**

**Figure (16) total temperature contours (K) at (P_o= 0.5 bar, T_o= 355.13 K) and
different back pressure ((a) P_b= 0.3 bar, (b) P_b= 0.21 bar, (c) P_b= 0.17 bar).**

253